UDC: 004.93 DOI: https://doi.org/10.15407/jai2022.01.311

3D-RECONSTRUCTION OF DESTRUCTIVE PROCESS MODELS USING REMOTE SENSING BY A GROUP OF UNMANNED AERIAL VEHICLES

V. Sherstjuk[1], M. Zharikova[2], I. Dorovskaja[3], D. Chornyi[4], V. Romantsov[5], N. Kozub[6], V. Gusev[7], I. Sokol[8]

[1, 2,3,4,5,6]Kherson National Technical University, Ukraine
24, Berislav Road, Kherson, 73025
vgsherstyuk@gmail.com
[7,8]Kherson State Maritime Academy, Ukraine
20, Ushakov Ave., Kherson, 73000
[1]http://orcid.org/0000-0002-9096-2582
[2]http://orcid.org/0000-0001-6144-480X
[3]http://orcid.org/0000-0001-5990-0992
[4]http://orcid.org/0000-0001-5323-5071
[5]http://orcid.org/0000-0002-5897-1809
[6]http://orcid.org/0000-0002-0406-0161
[7]http://orcid.org/0000-0001-7775-2276
[8]http://orcid.org/0000-0002-7324-1441

Abstract. The paper presents a novel method of volumetric reconstruction of transient destructive processes using remote sensing by a group of unmanned aerial vehicles. The study is based on the most common class of such processes like forest fires, where a fire front is a determinant, and its propagation reflects the dynamics of the process. The effects of wind, smoke and fire, turbulence and vibration, interference, distortion, and obstacles lead to uncertainty of observations, to overcome which fuzzy sets, soft sets and gray numbers were combined. A spatial model based on a recursive eight-fold subdivision of space as well as on a hierarchical structure of virtual cells is proposed, which allowed to resolve the contradictions between the accuracy and rate of reconstruction. The set of possible states of virtual cells is determined and the algorithm of their classification based on the use of a five-channel image recognition system containing infrared, two main, and two additional optical channels is proposed. An algorithm for calculating a 3D observation vector, presented by an array of confidence vectors, is proposed, which can be used to determine the gray fuzzy state of virtual cells allowing a combination of observations from different observers and refining them sequentially. The terrain where the process evolves is represented by a soft gray fuzzy set of virtual cells, which belong to a specific state at the consideration time, allowing identification of convincing, uncertain, suspicious, and negative components. The first one defines a stable core of the fire front while the second one represents its variation caused by uncertainty. The proposed method allows the reconstruction of transient spatially distributed processes of other classes, smoothing the effects of distortions and noise and ensuring acceptable performance.

Keywords: unmanned aerial vehicle, multi-view observation, uncertainty, image processing, fire front, virtual boxes, grey fuzzy soft set.

ВІДТВОРЕННЯ 3D-МОДЕЛЕЙ ШВИДКОПЛИННИХ ПРОЦЕСІВ РУЙНІВНОГО ХАРАКТЕРУ ЗА ДОПОМОГОЮ ДИСТАНЦІЙНОГО ЗОНДУВАННЯ ГРУПОЮ БЕЗПІЛОТНИХ ЛІТАЛЬНИХ АПАРАТІВ

В. Г. Шерстюк[1], М. В. Жарікова[2], І. О. Доровська[3], Д. О. Чорний[4], В. В. Романцов[5], Н. О. Козуб[6], В. М. Гусєв[7], І. В. Сокол[8]

[1,2,3,4,5,6]Херсонський національний технічний університет, Україна
Бериславське шосе, 24, м. Херсон, 73008
vgsherstyuk@gmail.com
[7,8]Херсонська державна морська академія, Україна
пр. Ушакова, 20, м. Херсон, 73000
[1]http://orcid.org/0000-0002-9096-2582
[2]http://orcid.org/0000-0001-6144-480X
[3]http://orcid.org/0000-0001-5990-0992
[4]http://orcid.org/0000-0001-5323-5071
[5]http://orcid.org/0000-0002-5897-1809
[6]http://orcid.org/0000-0002-0406-0161
[7]http://orcid.org/0000-0001-7775-2276
[8]http://orcid.org/0000-0002-7324-1441

Анотація. У статті представлено новий метод об’ємної реконструкції швидкоплинних руйнівних процесів за допомогою дистанційного зондування групою безпілотних літальних апаратів. Дослідження виконано на прикладі найпоширенішого класу таких процесів - лісових пожеж, де фронт вогню є детермінантом, а його рух відображає динаміку процесу. Вплив вітру, диму та вогню, турбулентність та вібрації, перешкоди, викривлення та спотворення призводять до невизначеності спостережень, для подолання якої було об’єднано нечіткі й м’які множини та «сірі» числа. Запропоновано просторову модель, засновану на рекурсивному восьмиелементному поділі простору та ієрархічній структурі віртуальних комірок, що дозволило вирішити протиріччя між точністю та швидкістю реконструкції. Визначено множину можливих станів віртуальних комірок та запропоновано алгоритм їх класифікації, заснований на використанні п'ятиканальної системи розпізнавання зображень, що містить інфрачервоний, два основних і два додаткові оптичні канали. Запропоновано алгоритм, що обчислює тривимірний вектор спостереження, поданий масивом векторів впевненості, за допомогою якого визначають сірий нечіткий стан віртуальних комірок, що дозволяє поєднувати спостереження від різних спостерігачів та послідовно їх уточнювати. Місцевість, де розвивається процес, подано м’якою сірою нечіткою множиною віртуальних комірок, які відносяться до певного стану на момент розгляду, що дозволяє визначити переконливий, невизначений, підозрілий та негативний компоненти. Перший з них подає стабільне ядро фронту вогню, а другий - його змінну, викликану невизначеністю спостережень. Запропонований метод дозволяє відтворювати швидкоплинні просторово-розподілені процеси й інших класів, згладжуючи ефекти спотворень і шумів при спостереженні та забезпечуючи прийнятну продуктивність.

Ключові слова: безпілотний літальний апарат, спостереження з багатьох точок, невизначеність, обробка зображень, фронт вогню, віртуальні комірки, сіра нечітка м'яка множина.

Introduction

The new millennium has brought the world a significant acceleration of climate change, population growth, increased urbanization and industrialization as well as many other negative consequences of human activities. The more intense and destructive for nature is the development of human civilization, the more nature responds to it by sufficient changes. Currently, the world is overloaded with natural disasters, from large-scale floods and forest fires to sudden earthquakes, tsunamis, tornadoes, and other natural features, which are often lined up in chains and accompanied by man-made disasters because of anthropogenic factors, human inattention, negligence etc [1].

Today, humanity has not adapted to climate change and has not created adequate methods for forecasting and preventing natural disasters, so it is mostly concerned with the localization and elimination of their consequences. Unfortunately, most of such phenomena are random, non-stationary, nonlinear, and unpredictable processes, which, moreover, develop very quickly in space and time and usually are not well observed [2]. However, the consequences of such phenomena - destruction of infrastructure, economic and environmental damage, degradation of natural objects, lost health, and even human lives - are very well observed.

Thus, given the fact that the considered natural phenomena can be represented by a class of transient dynamic spatially distributed processes of destructive nature, people cannot build acceptable mathematical models of such phenomena at the current level of science development. Due to the lack of reliable models, low observability, and increasing scale, speed, and intensity of natural disasters, the tasks of localization, response, and elimination the consequences of disasters become much more difficult for those involved because they must be solved with a high degree of responsibility, essential time constraints in the conditions of uncertainty and unpredictability. Since response operations are often based on visual observations, information support for decision-makers is crucially actual and therefore is the topic of our current interest.

Problem statement

The new era has brought humanity not only new challenges but also new opportunities related to the development of unmanned vehicles, remote sensing, image processing, machine learning, and other modern technologies. Unmanned aerial vehicles (UAVs) can best assist in monitoring the development of destructive processes "from above", which allows, on the one hand, to get as close as possible to the observed events, and on the other hand, keeping them at a safe distance [3]. The ability to observe "above" and "sideways" by UAVs allows a much wider coverage of spatially distributed

events, reaching a fundamentally different scale of situational awareness of decision-makers. Therefore, the use of UAVs is considered promising in many emergency monitoring systems, such as forest fires.

This paper will be devoted to the reconstruction of the forest fire development model as one of the most common classes of transient destructive processes. However, the opportunity of using UAVs in a broader sense is provided only by their equipping of certain sensors that allow assessing the value of certain measured parameters at certain points in the observation space. For example, optical and infrared cameras are relevant for forest fire monitoring, while level, humidity sensors are required for flood monitoring. Therefore, due to the above-mentioned advantages, UAVs equipped with relevant remote sensors can be a modern tool for monitoring a wide class of transient spatially distributed natural phenomena.

On the other hand, the observation of natural phenomena even by UAVs is always complicated by obstacles and distortions, so the accuracy of remote measurement of parameters needed is currently not ideal. For example, the effects of wind, smoke and fire, air turbulence, and UAV vibrations prevent accurate observing the forest fire propagation. In addition, there are certain spatial constraints, such as the multiplicity of fire spots, fire front segmentation, fuel and terrain variability, which makes it difficult to obtain a reliable image of the situation for planning and implementation of fire response operation by decision-makers.

An important advantage of a UAV is that it can observe the process moving, i. e., changing the point of view of the situation, and can approach a certain target point much closer than a human. However, due to the high combustion temperature, the observation point cannot be closer to the forest fire front than it is acceptable for UAV safety reasons, so it is impossible to overcome the uncertainty of observations and capture the process completely. Thus, the peculiarities of spatially distributed transient processes do not allow to fully observe the process from one observation point, even in the case of continuous UAV movement, therefore, the solution of the process reconstruction problem requires simultaneous observation from several different points [4]. When using multiple UAVs, the completeness of the observations is significantly added, but a problem of their incompatibility and inconsistency occurs.

It is known that decision-makers must be situationally informed to plan response operations, i. e., they must understand the process development, assess the directions and speed of fire spreading. Fortunately, they do not require over-detailed information but should be informed on the strength, directions, and speed of the fire front in time. Thus, when reconstructing a process by UAV surveillance, the most important limitation is the time required: the sooner the dynamics of the process are determined, the sooner the decision-maker will be able to plan a response operation.

Therefore, the problem addressed in this paper relates to the reconstruction of dynamic processes using multi-view observation by a group of UAVs. We will investigate the uncertainty conditions of joint remote sensing by multiple UAVs and the relevant issues.

Related works

There is always a certain determinant in each process that reflects its dynamics. For example, in the forest fire process, such a determinant is the fire front, which is formed under the influence of high-temperature combustion reaction and moves, leaving already burned areas where there is no fuel left for the combustion reaction, and covering new areas where fuel is available [5]. The stronger the fire, the higher and wider the fire front. Thus, the reconstruction of the forest fire process is a three-dimensional reproduction of the fire front according to the observations of fire signs at certain points in space, namely fire, flame, smoke, high temperature [6]. The presence of the first three signs can be recognized using optical cameras, and the fourth - using infrared cameras. In any case, it is necessary to use modern methods of computer vision and remote sensing to assess the fire front surface (contour) captured by sensors. This task is quite similar to the object recognition task. A three-dimensional model of an object can be reconstructed by scanning

its surface from several viewpoints sequentially. A detailed review of the object recognition methods is presented in [7]. Clearly, objects are usually implied static, but forest fire is an entirely dynamic process. Thus, well-known object recognition methods are generally insufficient [8], however, they provide a possibility of sequential recognition of the fire front position and state obtaining a model of its motion that reflects a process of fire propagation. The multi-view object reconstruction method has been proposed to overcome visibility constraints [9]. This approach allows scanning objects in real-time but is quite sensitive to sparse and uncertain observations.

A volumetric approach is almost closest to the subject of our consideration [10]. There are real 3D volumetric methods that describe objects by 3D point clouds, and 2.5D methods that describe only measured height (or depth) for a certain 2D area. Both 3D and 2.5D methods are oversensitive to sensor noises and cannot distinguish suspicious areas [11]. Obviously, a flame is a certain “eigenfeature” of the fire front with variable shape and color. Effects of smoke, wind, flares, and flickers, complicate the flame recognition significantly.

Thus, various distortions, interferences, and obstacles lead to many unrecognized and uncertain elements in the scanned image, so we need to assess some signs of fire (flame, smoke etc.) within certain areas by a degree of confidence based on the uncertain observations. The volumetric 3D method proposed in [6] uses a soft-rough uncertainty model to describe the fire front by a cloud of blurred 3D cells. Another approach is probabilistic, which represents uncertainty in terms of chances [12] but can deal only with stochastically stable data. That is why various non-probabilistic methods have been developed for image recognition tasks. The most widely used are fuzzy sets [13], which is a convenient tool to represent vague data by a membership degree of a certain element. Rough set [14] is also a tool to deal with imprecise or noisy data based on a relation of their indiscernibility, which allows approximating it by two crisp sets (lower and upper approximations).

Fuzzy sets mainly represent subjective uncertainties highlighting the vagueness of information while rough sets mostly represent objective uncertainties focusing on incomplete information. Both approaches complement each other perfectly and are therefore often combined. However, both have a common disadvantage - they need a priori information about the membership function or the indiscernibility relation, which cannot be obtained in advance during the reconstruction of the dynamic process.

A soft set [15] is a model of both uncertainties and vagueness determined through a certain parametrization of any kind that is free from a priori information inadequacies. Grey numbers [16] can also be an adequate model in cases when the exact value is not completely known. It introduces a certain set of values like intervals but represents only one of them.

Usually, the reconstruction of the forest fire front is performed under uncertain conditions of various nature, which cannot be modeled by incomplete, inaccurate, or vague information separately. Degrees of confidence are spatially distributed and dynamic, while the observation space is sufficiently sparse and contains many uncertain and suspicious areas. Since fuzzy, rough, soft, and grey models are closely related and complementary to each other [17], it is appropriate to combine them into a certain complex model reflexing both objective and subjective uncertainty.

Thus, despite the overall progress in the fields of object reconstruction and image processing in the conditions of uncertainty, many of their issues have a little reflection in the literature, remain insufficiently investigated, and need further research.

The aims of the paper

Considering the above-mentioned reasons, the process reconstruction task must be solved using three-dimensional (volumetric) multi-view observations taking into account their incompleteness, uncertainty, and inconsistency. Thus, the most topical issue for today is the investigation of approaches to the 3D reconstruction of dynamic processes based on the example of forest fires. The paper aims to propose a proper method for 3D reconstruction of the forest fire front based on

uncertain multi-view observations by a group of UAVs considering their distortions, interferences, and noises.

Methodology

The main idea is that the signs of fire (flame, smoke etc.) observed in certain spatial areas can be assessed by certain degrees of membership in the corresponding class of spatial areas. Since the observation space is sparse and observations are mainly incomplete, various uncertain, undefined, or suspicious areas can also be approximated by certain degrees of confidence. Due to the simultaneous effects of several uncertainties of different nature, we need to combine fuzzy, soft sets, and "gray" numbers in the complex uncertainty model.

A. Reconstructed scene

The multi-view observation of the forest fire by a group of UAVs is depicted in fig. 1.

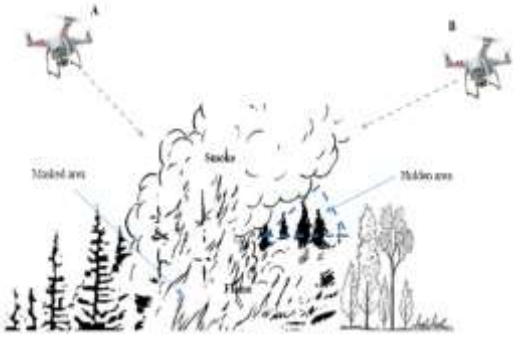

Fig. 1. Multi-view fire front monitoring

Clearly, the fire front can be determined by signs of flame. However, the smoke masks the flame, and the wind makes them dynamic.

The reconstructed scene is defined as a configuration of poses as shown in fig. 2. The pose is a viewpoint, in which spatial position is determined by geolocation of UAV and orientation of its sensors. The last is usually chosen according to the horizontal and vertical normal to the image plane. Each pair of poses enables a stereoview.

Based on the known UAV's geolocation in each stereo-pair and relative geometry of their poses, the depth of the scene can be perceived and, accordingly, the geolocation of spatial elements observed from the specified poses can be evaluated. A certain spatial model can be used to define spatial elements.

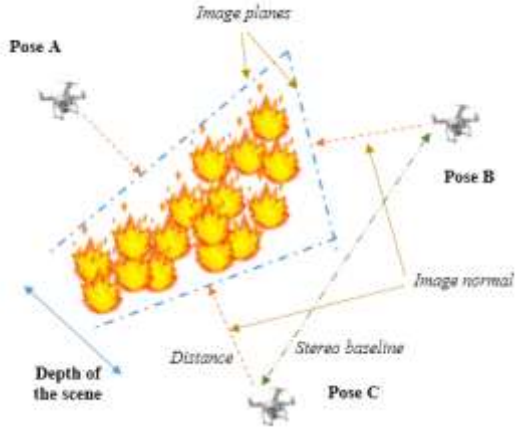

Fig. 2. The reconstructed scene

B. The Spatial model

Discrete spatial models are most often used to solve recognition tasks; in the case of three-dimensional objects recognition, three-dimensional Euclidean space must be discretized by cubic cells. Thus, we can traditionally use isometric cubic cells d_{xyz} having the size $\delta \times \delta \times \delta$. Consequently, the terrain where the forest fire spreads can be represented by three-dimensional space C discretized by a grid $D = \{d_{xyz}\}$ of cells d_{xyz} indexed along the axis X, Y, and Z.

The simplicity of this approach has a downside causing the main drawback. Since the fire front moves, leaving already burned areas where there is no fuel left for the combustion reaction and covering new areas where fuel is available, the grid D should be extended with new rows and columns dynamically every time as the fire front covers new areas. As well, rows and columns, which correspond to the burned-out areas, should be removed from the grid. In general, this poses two problems. First, we need to build an initial space of the maximum possible size to provide the possibility of developing a spatially distributed forest fire process to the maximal boundaries, which are not initially known. There is not only a problem of limiting the memory amount here but also the problem of significantly reducing performance due to excessively large dimensions of space. Second, each cell requires geo-localization and geo-reference during image processing that slows down the fire front reconstruction at a high rate of fire propagation, which often happens. The higher the accuracy of the

sensors, the smaller the cell size, and the greater the drop in performance due to their excessive number.

To resolve the contradiction between the accuracy of the fire front reconstruction process and its speed, we need to build a spatial model that contains mainly the set of cells, which currently correspond to the spatial location of the fire front or close areas. Obviously, this can significantly reduce the number of cells to be processed. To do this, we can organize cells not only in the grid D but also in a virtual hierarchical structure I well-known as octree (fig. 3) [18].

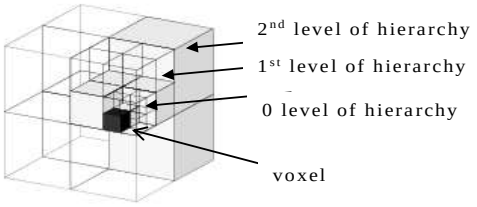

Fig. 3. Octree-based spatial structure [18]

An octree I is based on the principle of recursive eight-fold subdivision of spatial areas and represents a certain octant of nodes at each k-th level of the hierarchy, which can be defined by a tuple $I_k = \langle \perp_k, G_k, \prec_k \rangle$, where G_k is a set of nodes, $\prec_k$ is a partial inclusion order over G_k, and $\perp_k$ is the least element of $\prec_k$. Then, each node $g_l \in G_k$ represents a *virtual box* as a certain cubic volume. Splitting some node g_l of level k recursively, we can define another octant of sub-nodes (e.g., sub-boxes) of smaller size at a lower $(k-1)$ level of the octree I. Such recursion can be applied top-down or bottom-up. If 0 is the lowest level of I, a smaller virtual box $g_q \in G_0$ can be represented by a certain cell d_{xyz} of the grid D. To implement hierarchical structure I, we use a revised version of the OctoMap library, in which all nodes of the Octree have been supplemented by a feature vector (Fig. 4), which presents bitwise the generalized state of the nested sub-boxes in terms of signs of fire and smoke.

Hence, we get the opportunity to consider the fire front as a 3D set F of virtual boxes $\{g_1, \ldots g_j\} \in G_\iota$ at the certain hierarchy level ι of the octree I, each of which can be recursively subdivided down-fold to the cell level. If the fire covers a new area, we add a new $(\iota+1)$ level on the top of I considering the ι-th level as one of its sub-nodes. If some areas have been burnt, the correspondent node links can be simply eliminated from I.

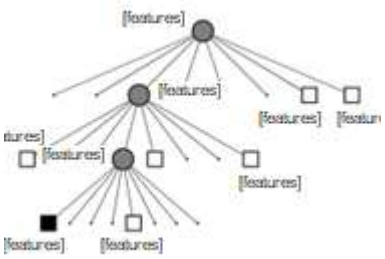

Fig. 4. The hierarchical structure of virtual boxes

C. State of the virtual box

Let $\Omega = \{\omega_1, \ldots \omega_7\}$ be a set of possible states of virtual boxes (table 1).

Table 1. States of virtual boxes

Class	*Function*	*Correspond to*
ω_1	Empty	"Free of fire" areas
ω_2	Flame	Areas having signs of flame
ω_3	Smoke	Areas having signs of smoke
ω_4	Burnt	Areas, which are already burnt
ω_5	Fuel	Vegetation areas ready to burn
ω_6	Uncertain	Uncertain or suspicious areas with respect to their burning state
ω_7	Unknown	Occluded areas or areas, which have not been seen by sensors

The "empty" state (ω_1) corresponds to virtual boxes that lie directly between the sensor and the surface represented by flame and smoke and define "free of fire" areas. The signs of flame (ω_2) means that the virtual box corresponds to a "fire surface" as well as the signs of smoke (ω_3) means attribute the virtual box to a "smoke cloud", both cases with a considerable degree of confidence. The "burnt" state (ω_4) corresponds to virtual boxes, which contain already burnt surfaces and, therefore, cannot be involved in the combustion processes in the future. The "fuel"

state (ω_5) corresponds to vegetation-covered virtual boxes, which at this time do not participate in the combustion processes but can be ignited due to readiness of the fuel. The areas, which do not contain any flammable vegetation, belong to the class ω_1 instead of ω_5.

The "uncertain" state (ω_6) corresponds to virtual boxes, which cannot be reliably classified into the classes of state ω_1-ω_5 based on the data captured by sensors. Such virtual boxes are mainly consistent with suspicious areas possibly involved in the combustion process but there is not enough confidence due to the uncertain observations. The "unknown" state (ω_7) corresponds to both virtual boxes occluded by boxes of other classes, which prevent the perception of the fire front, and virtual boxes, which have not been seen by sensors.

Initially, the reconstruction scene is represented by a 3D set of virtual boxes marked by an "unknown" state. Depending on the result of image processing, each virtual box must be matched to a certain class $\omega_i \in \Omega$. Obviously, the virtual boxes of a ω_2-class correspond to clearly observable inner boundaries ("burning kernel") of the fire propagation process, the virtual boxes of a ω_3-class correspond to a "smoke cloud", i. e. the areas around the fire front shrouded in smoke, which masks "surface" of the fire front and prevents its confident recognition, and the virtual boxes of ω_6-class correspond to areas, which, for various reasons, are poorly observed or about which there are doubts due to inaccuracy, inconsistency, or incompatibility of observations from different viewpoints. The virtual boxes of the classes ω_4 and ω_5 represent clearly visible outer boundaries of the fire propagation process. Blurred, uncertain, or underdetermined areas, which dynamically change because of wind, smoke, and other factors, lie between the clearly observed inner and outer boundaries of the fire propagation process. Of course, during the reconstruction, all virtual boxes, which state cannot be clearly and reliably determined in the range ω_2-ω_6, are identified as "free of fire" (ω_1), as well as all virtual boxes, which cannot be observed by sensors for various reasons, remain in a state "unknown" (ω_7).

D. Image processing

To classify virtual boxes according to table.1, we can use a multi-channel image recognition system (fig. 5).

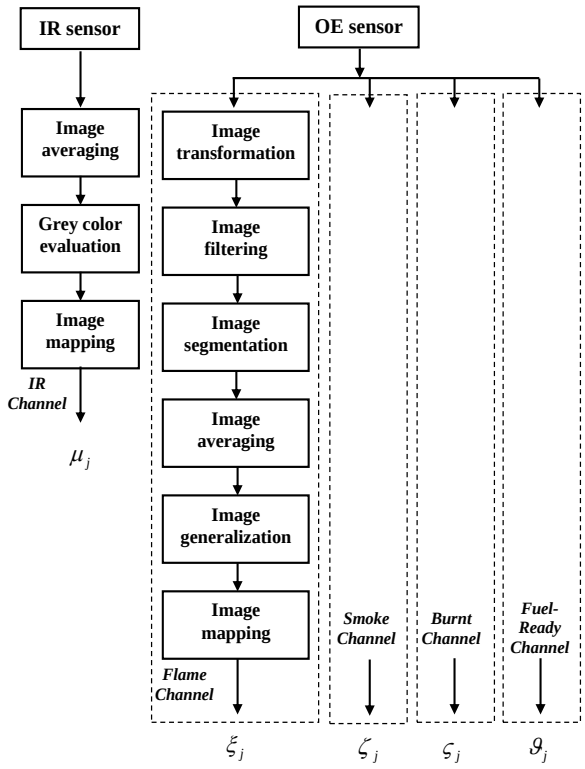

Fig. 5. Image processing

The infrared channel is reliable in nighttime and under heavy smoke because of the infrared transparency of the latter, but in the daytime, it has too small contrast, therefore, images can be affected due to reflected sunlight, saturation etc. Heat radiation can be determined in captured images by the color of pixels, which changes from black to white depending on the heating level. Although combustion is always represented by pixels of close-to-white colors while free of fire areas are always black, due to imprecise, uncertain, or ambiguous measuring in the daytime, unfortunately, most of the pixels are in different shades of gray. Thus, in the infrared channel, image processing is performed in three stages: *image averaging*, *gray color evaluation*, and *image mapping* [5]. At the output of the last stage, each defined virtual box g_i is associated with a certain "degree of grayness" μ_j calculated

based on the average brightness B_j of the corresponding pixels in the captured image and mapped to the range [0, 1].

Based on the images captured by optical cameras, two main optical channels provide flame [19] and smoke [20] recognition separately. Both channels work identically based on the *HSI* color model, but they have different settings. In the flame recognition channel, the conventional fires correspond to colors from dark red to light yellow color with high saturation and profiles $\rho_1 = [0° - 60°, 0.4 - 1.0, 0.5 - 1.0]$ in the daytime and $\rho_2 = [0° - 60°, 0.2 - 0.85, 0.5 - 1.0]$ in the nighttime or in bad weather conditions. The well-developed fires correspond to colors from light blue to white with high saturation and profiles, respectively, $\rho_3 = [220° - 260°, 0.4 - 1.0, 0.5 - 1.0]$ and $\rho_4 = [220° - 260°, 0.2 - 0.85, 0.5 - 1.0]$ respectively [21]. In the smoke recognition channel, the intensity is high, saturation is low, and colors are mainly gray and silver, so the profiles are defined, respectively, as $\rho_5 = [355° - 5°, 0 - 0.05, 0.5 - 0.85]$ and $\rho_6 = [230° - 240°, 0 - 0.05, 0.5 - 0.85]$. For this reason, in the flame recognition channel, the center colors are bright orange ($\pi_1 = [30°, *, *]$) and blue ($\pi_2 = [240°, *, *]$) while in the smoke recognition channel the center colors are silver ($\pi_3 = [235°, *, *]$) and white ($\pi_3 = [0°, *, *]$) [22].

The other two optical channels are auxiliary and developed to recognize burnt and fuel-ready areas. They work in a similar way to the above-mentioned main channels, but their profiles are different. The first of them is characterized by low values of intensity (in the range [0-0.25]) for any values of hue and saturation.

The second one is determined mainly by light green color tones; however, the channel's settings may vary significantly in different areas of different climatic zones. In Southern Ukraine, the profile $\rho_5 = [100° - 120°, 0.3 - 0.75, 0.1 - 0.8]$ is the most appropriate.

In the optical channels, the image processing is performed in the following sequential stages:

- *image transformation*: to convert each pixel of the image from *RGB* to *HSI* color model and normalize all components to the ranges $0 \le H \le 360°$, $0 \le S \le 1$, and $0 \le I \le 1$. After that, the intensity and saturation components are separated from the color components to speed up the next stages.
- *image filtering*: the pixels, which *HSI* values do not match the proper ranges for the filters $(\rho_1 - \rho_6)$, should be eliminated and their colors should be replaced by the rose color to speed up the next stages.
- *image segmentation*: based on the color feature and the raster scanning algorithm, the image is divided into certain rectangular areas (segments) [23].
- *image averaging*: the *H*, *S*, and *I* values of pixels are averaged to the mean values H_l, S_l, and I_l within each l-th segment.
- *image generalization*: for each l-th segment, it calculates the degree of similarity to the closest center color in the range [0, 1] based on the mean values H_l, S_l, I_l.
- *image mapping*: the image is oriented, transformed, and then all its segments are mapped to the uniquely corresponding virtual boxes.

After the image segmentation stage, due to the non-linearity and incompleteness of the observations, four-layer fully connected backpropagation neuron networks, which consists of the input, two hidden, and the output layers, are used in image processing in four optical channels to improve the accuracy and reliability. The network architecture is 15×18×6×1. The input data is the *H*, *S*, and *I* value of pixels of three last consecutive image frames (*i*-1, *i*, *i*+1). Besides that, the features of bad weather *W* and daytime *D* are also used as inputs. The transfer functions are defined as log-sigmoid at the input and first hidden layers, and as the Gauss-based radial basis function at the second hidden layer. The number of the hidden layers and hidden nodes have been experimentally evaluated. The output is the degree of similarity of the input to the corresponding samples.

At the final stage, each j-th virtual box g_j is connected to a certain confidence vector $\Xi_j = \left[\mu_j, \xi_j, \zeta_j, \varsigma_j, \vartheta_j\right]$, where μ_j is the degree of greyness, ξ_j, ζ_j, ς_j, and ϑ_j are degrees of similarity in respectively flame, smoke, burnt and fuel-ready channels. All elements of Ξ_j are normalized in the range [0, 1].

Considering the structure I as a simple set of virtual boxes, $I = \left\{g_j\right\}_{j=0}^{m}$, we define a 3D observation vector Ξ as a correspondent array of confidence vectors, $\Xi = \left|\Xi_j\right|_{j=0}^{m}$.

E. Classification of virtual boxes

Let $\mathrm{B} = \left\{\beta_1, \beta_2, \beta_3\right\}$ be a set of threshold values and $\Lambda = \left\{\lambda_1, \lambda_2, \lambda_3, \lambda_4\right\}$ be a set of factors defined such that $\lambda_1 + \lambda_2 = 1$ and $\lambda_3 + \lambda_4 = 1$.

The classification of virtual boxes concerning the set of states Ω and the 3D observation vector Ξ is performed in four following stages (fig. 6).

At the first stage (*scene analysis*) we divide the 3D observation vector Ξ into foreground and background areas using the threshold values $\beta_i \in \mathrm{B}$. Thus, the background area contains all virtual boxes g_b that $\xi_b \le \beta_1$, the foreground area contains all virtual boxes g_f that $\xi_f \ge \beta_2$, and the suspicious area contains all virtual boxes g_s such that $\zeta_s \le \beta_3$.

At the second stage (*flame confidence clarification*), based on the set of factors Λ as well as «day/night» and weather features, we clarify the flame confidence η_j for each virtual box g_j related to foreground or suspicious areas. In the daytime and under good weather conditions, the foreground cells' flame confidence is $\eta_j = \xi_j$ while suspicious cells' flame confidence is $\eta_j = \lambda_1 \cdot \mu_j + \lambda_2 \cdot \xi_j$. In the nighttime and under bad weather conditions, the foreground cells' flame confidence is $\eta_j = \lambda_3 \cdot \mu_j + \lambda_4 \cdot \xi_j$ while suspicious cells' flame confidence is $\eta_j = \mu_j$. In most cases, the factor's values $\lambda_1 = -\zeta_j$ and $\lambda_4 = \zeta_j$ is convenient. As a result, we substitute the couple μ_j and ξ_j by the flame confidence η_j in all confidence vectors $\Xi_j \in \Xi$.

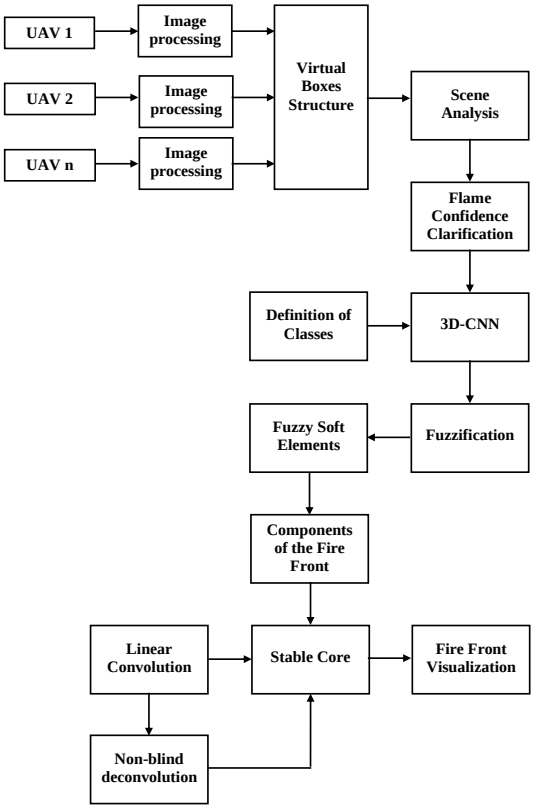

Fig. 6. Classification of virtual boxes

At the next stage, we classify virtual boxes $I = \left\{g_j\right\}_{j=0}^{m}$ concerning the 3D observation vector Ξ using a 3D convolutional neural network (3D-CNN), which is a special kind of CNNs based on 3D volumes in the kernels instead of 2D maps. We use VoxNet [24] 3D-CNN architecture (fig. 7). Its convolutional layers are based on 128 features, 5×5×5 kernel, 2×2×2 stride, and 2×2×2 max-pooling operation (C1), 32 features, 4×4×4 kernel, 2×2×2 stride, and 2×2×2 max-pooling operation (C2), 8 features, 3×3×3 kernel, 2×2×2 stride, and 2×2×2 max-pooling operation (C3). Fully connected layers FC1, FC2, FC3 are based on 1200, 400, and 32 parameters respectively. The output is defined as a confidence vector $C_j = \left\langle \alpha_{j1}, \ldots \alpha_{j7} \right\rangle$, where α_{ji} is a degree of confidence that the virtual box g_j is in the state ω_i, $\alpha_{ji} \in [0,1]$.

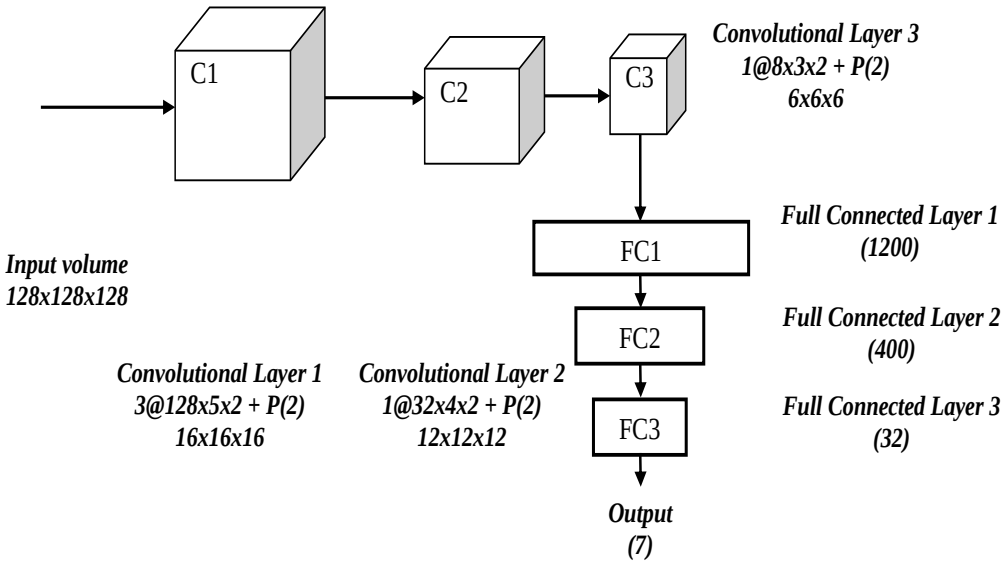

Fig. 7. 3D-CNN Architecture

Let $\Phi = \{\tilde{\varphi}_i\}_{i=1}^{7}$ be a family of fuzzy sets $\tilde{\varphi}_i$, each of which contains all virtual boxes $g_j \in I$, the state of which is ω_i.

At the final stage, we do fuzzification to decompose the output of 3D-CNN into fuzzy sets of a family Φ. Thus, using the triangular-shaped membership functions, the degrees of membership to which the certain virtual box g_j belongs to each given fuzzy set $\tilde{\varphi}_i \in \Phi$ should be determined.

F. Reconstruction process

Let U be a set of UAVs jointly observing the terrain, where a forest fire dynamic process is developing. Suppose each UAV $U_j \in \mathrm{U}$ is located at a distinctive viewpoint. Let T be a linear ordered timescale such that $t_{m+1} > t_m$.

Let I be a spatial model of the considered terrain represented by the hierarchical structure of virtual boxes denoted by g_{lqi}, where l is the level of the virtual box g_{lqi} in the hierarchy I, q is a connection to the comprising virtual box of level $l+1$, and i is a number of the virtual box within the comprising virtual box (from 1 to 8).

Let $\tilde{\gamma}_{lqijkt}$ be a degree of membership to which the lqi-th virtual box belongs to the fuzzy set $\tilde{\varphi}_i$ of virtual boxes being in the state ω_k from the viewpoint of $U_j \in \mathrm{U}$ at the moment $t \in T$.

Thus, a fuzzy state $\bar{g}_{lqijt}$ of the virtual box g_{lqi} visible from UAV U_j at the moment t is a vector

$$\bar{g}_{lqijt} = \left(\left\langle \tilde{\gamma}_{lqij1t}, \omega_1 \right\rangle, \ldots \left\langle \tilde{\gamma}_{lqij7t}, \omega_7 \right\rangle\right), \qquad (1)$$

where g_{lqi} and $\tilde{\gamma}_{lqijkt}$ are defined as above, $\omega_1, \ldots \omega_7 \in \Omega$ are the states defined in table 1.

Since the purpose of multi-view observation is to capture images of the target same areas from different positions simultaneously, several UAVs are watching the process development differently from different viewpoints. Certain areas of the terrain are better visible to one UAV, but others see it worst, so the first one has more confidence than others. Moreover, their information can be inconsistent; the accuracy and completeness of observation can also vary. Given the fact that UAVs most often move during the observation, the information is usually dynamic, so the confidence and accuracy of observation may increase at some points while decreasing at other points.

Clearly, we need a reasonable way to combine uncertain observations of the same virtual box from different viewpoints and clarify them during continuous observation. A hesitant multi-fuzzy set [25] can be used to combine observations from different observers

$U_1,...U_n$. Thus, a multi-view fuzzy state $\tilde{\tilde{g}}_{lqit}$ of the virtual box g_{lqi} by UAVs $U_1,...U_n$ at the moment t can be represented as

$$\tilde{\tilde{g}}_{lqit}=\begin{pmatrix}\left\langle \omega_1,\left(\tilde{\gamma}_{lqi11t},...\tilde{\gamma}_{lqin1t}\right)\right\rangle,... \\ \left\langle \omega_7,\left(\tilde{\gamma}_{lqi17t},...\tilde{\gamma}_{lqin7t}\right)\right\rangle\end{pmatrix}. \quad (2)$$

There is a 7-elements array of classes ω_i, each of which is defined by the correspondent fuzzy set of virtual boxes $\tilde{\varphi}_i$ and represented by an array of *n* degrees of membership to this set concerning *n* different observers. All these membership degrees lie on the interval between their minimum and maximum values. Such intervals can be consequently narrowed during continuous observations. Thus, (2) can be transformed to:

$$\tilde{\tilde{g}}_{lqit}=\begin{pmatrix}\left\langle \omega_1,\begin{bmatrix}\min\left(\tilde{\gamma}_{lqi11t},...\tilde{\gamma}_{lqin1t}\right), \\ \max\left(\tilde{\gamma}_{lqi11t},...\tilde{\gamma}_{lqin1t}\right)\end{bmatrix}\right\rangle, \\ ...\left\langle \omega_7,\begin{bmatrix}\min\left(\tilde{\gamma}_{lqi17t},...\tilde{\gamma}_{lqin7t}\right), \\ \max\left(\tilde{\gamma}_{lqi17t},...\tilde{\gamma}_{lqin7t}\right)\end{bmatrix}\right\rangle\end{pmatrix} \quad (3)$$

without loss of accuracy.

Suppose $\beta^{-}_{lqikt}=\min\limits_{j=1..n}\left(\tilde{\gamma}_{lqijkt}\right)$ and $\beta^{+}_{lqikt}=\max\limits_{j=1..n}\left(\tilde{\gamma}_{lqijkt}\right)$, $k=[1,7]$. The above-mentioned intervals can be further defined as

$$\beta^{\pm}_{lqikt}=\left[\beta^{-}_{lqikt},\beta^{+}_{lqikt}\right]. \quad (4)$$

Such definition corresponds exactly to grey numbers [16]. Given this fact, we can define a grey fuzzy state of the virtual box g_{lqi} at the moment t based on (3) and (4) as:

$$\hat{\tilde{g}}_{lqi}=\left(\left\langle \omega_k,\beta^{\pm}_{lqikt}\right\rangle_{k=1}^{7}\right) \quad (5)$$

Let $\succ$ be a partial order (preference) relation induced on the set of possible states Ω of virtual boxes, such that $\omega_1\succ\omega_2\succ\omega_3\succ\omega_4\succ\omega_5\succ\omega_6\succ\omega_7$. This relation allows determining the class *i* of the virtual box in the case of approximate equality of some membership degrees by the selection of the most trusted of them:

$$\hat{\tilde{g}}_{lqit}=\left(\omega_z,\beta^{\pm}_{lqizt}\right) \text{ if } \omega_z\succ \textit{all other } \omega_k.$$

G. Fire front representation

Let the virtual structure I be a universe. Suppose Ω is a parameter set. Let Y be a mapping of Ω into a set of all possible subsets of virtual boxes of I. A pair (Y,Ω) can be considered as a soft set Υ of virtual boxes over I [15]. In this case, the soft set $\Upsilon=(Y,\Omega)$ is a family of certain subsets of the hierarchical set of boxes I parameterized by the elements of the set Ω, i. e., by the specific states of the virtual boxes. Hence, $Y(\omega_k,t)$ is considered as a ω_k-approximate element of the soft set of the virtual boxes being in the state $\omega_k\in\Omega$ at the moment $t\in T$. Therefore, Y is a dynamic mapping and the correspondent soft set is also dynamic, so it can represent the dynamics of the observed process. We regard the soft set Υ consisting of 7 elements as below:

$$\Upsilon=\left\{\left(\omega_k,Y(\omega_k,t)\right):\omega_k\in 2^{\Omega},Y(\omega_k,t)\in 2^{I}\right\}_{k=1}^{7}.$$

Suppose the grey number $\beta^{\pm}_{kt}$ defined as $\left[\beta^{-}_{kt},\beta^{+}_{kt}\right]$ represents the degree $\hat{\gamma}_{kt}$ of the virtual box membership in the ω_k-approximate element of the soft set Υ, i. e. the set of the virtual boxes being in the state $\omega_k\in\Omega$ at the moment of the process reconstruction $t\in T$. In this case, a mapping of Ω into the set of virtual boxes of I must take into account their membership degree, so the elements of the soft set can be defined as $\hat{Y}(\omega_k,t,\hat{\gamma}_{kt})\to([0,1],[0,1])$ and the pair $\left(\hat{Y},\Omega\right)$ defines a soft grey fuzzy set $\hat{\Upsilon}$.

Let (τ_{1k},τ_{2k}) be a pair such that $\tau_{1k},\tau_{2k}\in[0,1]$, $\tau_{1k}\le\tau_{2k}$. Using these numbers as thresholds we can divide each element of the soft grey fuzzy set $\hat{\Upsilon}$ into certain components. With respect to the ω_k-element of the soft grey fuzzy set $\hat{\Upsilon}$, the first component is a lower approximation $\underline{\hat{Y}}_k(t)=Y\left(\omega_k,t,[\hat{\gamma}_{kt}\ge\tau_{2k}]\right)$ that contains the virtual boxes definitely belonging to this element, the second one is an upper approximation $\hat{\bar{Y}}_k(t)=Y\left(\omega_k,t,[\hat{\gamma}_{kt}\ge\tau_{1k}]\right)$ that contains virtual boxes most likely belonging to this element, such that $\hat{\bar{Y}}_k(t)\subseteq\underline{\hat{Y}}_k(t)$, the difference $\hat{Y}_k(t)=\underline{\hat{Y}}_k(t)-\hat{\bar{Y}}_k(t)$ between them is a vague boundary that contains doubtful virtual boxes, and $\hat{\bar{Y}}_k(t)=Y\left(\omega_k,t,[\hat{\gamma}_{kt}\le\tau_{1k}]\right)$ is a negative region that contains virtual boxes,

which most likely do not belong to the ω_k-element.

The fire front F is defined using the following assumptions. Due to the dynamics of the forest fire and the effects of wind, terrain, and a wide range of distortions, interferences, and noises the observed states of the virtual boxes are dynamic and principally uncertain. Therefore, the fire front reconstruction can be performed by the uncertain distribution of the virtual boxes over the following components.

The *convincing component* F^+ represents the stable kernel of the fire front defined by the lower approximation of the ω_2-element $\underline{\hat{Y}}_2(t)$ of $\hat{\Upsilon}$, $F^+(t)=\underline{\hat{\Upsilon}}_2(t)$.

The *negative component* F^- contains virtual boxes, which should be confidently excluded from the fire front during the reconstruction, and is defined as the union of the lower approximations of the ω_1-, ω_4-, ω_5-, ω_6- and ω_7-elements of $\hat{\Upsilon}$, $F^-(t)=\underline{\hat{Y}}_1(t)\cup\underline{\hat{Y}}_4(t)\cup\underline{\hat{Y}}_5(t)\cup\underline{\hat{Y}}_6(t)\cup\underline{\hat{Y}}_7(t)$. In order to reduce the computations, ω_1- and ω_7-elements may not be approximated, then $F^-(t)=\hat{Y}_1(t)\cup\underline{\hat{Y}}_4(t)\cup\underline{\hat{Y}}_5(t)\cup\underline{\hat{Y}}_6(t)\cup\hat{Y}_7(t)$. If necessary, the same simplifications may apply to the ω_4- and ω_5-elements, moreover, the ω_1- and ω_7-elements may not even be grayed. In this case, $F^-(t)=Y_1(t)\cup\underline{\hat{Y}}_4(t)\cup\hat{Y}_5(t)\cup\hat{Y}_6(t)\cup Y_7(t)$.

The *uncertain component* F^* represents the variable component of the fire front defined by the union of the vague boundaries of the ω_2- and ω_4-elements and the lower approximation of the ω_3-element of $\hat{\Upsilon}$, $F^*(t)=\overline{Y}_2(t)\cup\underline{\hat{Y}}_3(t)\cup\overline{Y}_4(t)$.

The *suspicious component* $F^:$ of the fire front is defined by the vague boundaries of the ω_3-, ω_5-, ω_6-, ω_7-elements, and, if applicable, ω_1- element of $\hat{\Upsilon}$, $F^: =\overline{Y}_1(t)\cup\overline{Y}_3(t)\cup\overline{Y}_5(t)\cup\overline{Y}_6(t)\cup\overline{Y}_7(t)$.

Thus, the soft grey fuzzy model of the fire front $\hat{F}$ can be defined as $\hat{F}=F^+\cup F^*\cup F^:\cup F^-$.

Let $\Delta t=t_{i+1}-t_i$, $t_i,t_{i+1}\in T$ be a step of observation. Assume that the noise model is Poisson. Suppose the initial kernel of the fire front is determined by a statistically continuous part of the convincing component $F^+(t)$. Since the fire front is vague and not stable, we use a linear time-invariant convolution [26] to find its stable kernel F^Θ with a certain latent L and noise N. Thus, $F^+(t)=F^\Theta\otimes L+N$. The gradient method increases the kernel after each next step, be used. Then, a non-blind deconvolution method [27] can be performed to improve the kernel determined in the previous step.

The pair (τ_{1k},τ_{2k}) sets certain thresholds on the confidence for each ω_k-element of the soft grey fuzzy set $\hat{\Upsilon}$ and can vary due to the dynamics of the process. Their values can be determined during the continuous observation within each subsequent step by the integral of the minimum and maximum values, i. e., $\tau_{1k}=\int_{t_i}^{t_i+\Delta t}\min_{j=1..n}(\tilde{\gamma}_{lqijkt})$, $\tau_{2k}=\int_{t_i}^{t_i+\Delta t}\max_{j=1..n}(\tilde{\gamma}_{lqijkt})$.

Implementation

The proposed method has been experimentally implemented using Visual C++, OctoMap framework, ConvNet, and FANN libraries. The software prototype has been tested on a PC network (Pentium i7-10700 2.9 GHz, 32 Gb RAM, 512 Gb SSD).

Computer simulation results show that the proposed method allows reconstructing the fire front during multi-view observation by several UAVs representing its stable core (flame) in red colors, the variable component in shades of orange, the smoke in pink colors, the uncertain components in yellow, and the negative component in shades of blue. Fig. 8 depicts a visualization of the fire front.

The accuracy and the rate of the reconstruction has been evaluated during the experiment. Fig. 9 shows the accuracy of the reconstruction depending on the number of observers (UAVs) and the scale of the terrain model represented by the average size of the least virtual boxes. Fig. 10 shows the average time of the reconstruction of the fire front depending on the same parameters.

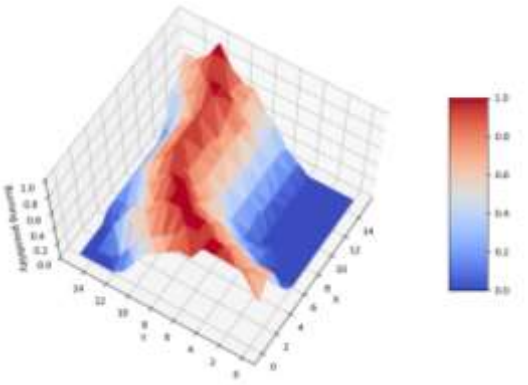

Fig. 8. Visualization of the forest fire front

Based on the experimental results, we concluded that the proposed method of the volumetric reconstruction of the fire front provides enough credibility to the decision-maker and sufficient performance to meet the requirements of the dynamic process reconstruction in real-time.

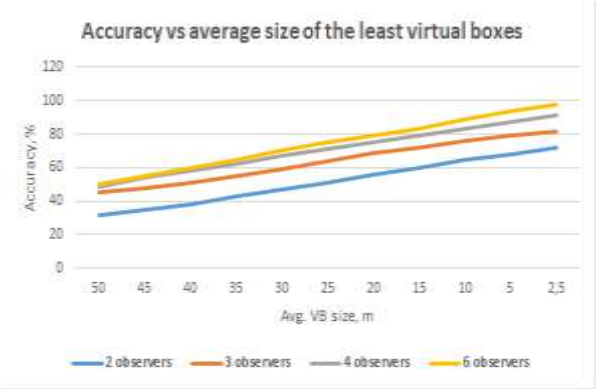

Fig. 9. Evaluation of Accuracy

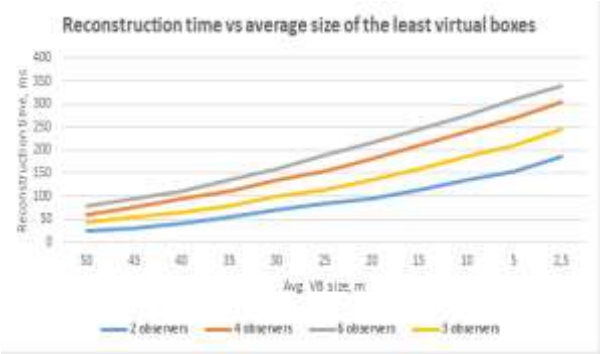

Fig. 10. Evaluation of Reconstruction time

Conclusion

The paper presents a novel method of the volumetric reconstruction of the forest fire front based on uncertain multi-view observations by a group of UAVs. The proposed method provides high performance due to a high-speed spatial model based on a virtual box hierarchy, which allowed to exclude iterative geo-localization and geo-rectification processes from the main image processing stage. The fire front representation is based on the fuzzy, soft sets, and grey numbers, which allowed to smooth the effects of distortions, interferences, and noises during the observation. The proposed approach ensures the possibility to reconstruct other classes of transient spatially distributed destructive processes if UAVs are equipped with suitable sensors and if the adequate classification of the spatial elements' states is defined. Further studies will be devoted to the blurring of spatial elements to improve the compatibility of multi-view observations and the optimization of the scene concerning the optimal location of observers to provide a more accurate reconstruction of the process.

References

1. Shen, G., Zhou, L., Wu, Y., Cai, Z. (2018). A global expected risk analysis of fatalities, injuries, and damages by natural disasters. Sustainability 10(7), 2573. https://doi.org/10.3390/su10072573.
2. Newman, J., Maier, H., Riddell, G., Zecchin, A., Daniell, J., Schaefer, A., van Delden, H., Khazai, B., O'Flaherty, M., Newland C. (2017). Review of literature on decision support systems for natural hazard risk reduction: current status and future directions. Env. modeling & software 96(C), 378–409. https://doi.org/10.1016/j.envsoft.2017.06.042.
3. Yuan, C., Liu, Z., Zhang, Y. (2017). Aerial images–based forest fire detection for firefighting using optical remote sensing techniques and unmanned aerial vehicles. J. Intel. & Robotic Syst. 88, 635–654. https://doi.org/10.1007/s10846-016-0464-7.
4. Merino, L., Martínez de Dios, J., Ollero, A. (2015). Cooperative Unmanned Aerial Systems for Fire Detection, Monitoring, and Extinguishing. In: Valavanis K., Vachtsevanos G. (eds) Handbook of Unmanned Aerial Vehicles, pp. 2693–2722. https://doi.org/10.1007/978-90-481-9707-1_74.
5. Sherstjuk, V., Zharikova, M., Dorovskaja, I., Sheketa, V. (2020). Assessing Forest Fire Dynamics in UAV-Based Tactical Monitoring System. In: Babichev, S., Lytvynenko, V., Wojcik, W., Vyshemyrskaya, S. (eds) Advances in Intelligent Systems and Computing 1246, 285–301. https://doi.org/10.1007/978-3-030-54215-3_18.
6. Sherstjuk, V., Zharikova, M., Dorovskaja, I. (2020). 3D Fire Front Reconstruction in UAV-Based Forest-Fire Monitoring System. In: Proc. of IEEE Third International Conference on Data Stream Mining & Processing (DSMP), pp. 243–248. https://doi.org/10.1109/DSMP47368.2020.9204196.
7. Mendez, O., Hadfield, S., Pugeault, N., Bowden, R. (2017). Taking the Scenic Route to 3D: Optimising Reconstruction from Moving Cameras. In: 2017

IEEE Int. Conf. on Computer Vision (ICCV), Venice, pp. 4687–4695. https://doi.org/10.1109/ICCV.2017.501.
8. Scott, W.R., Roth, G., Rivest, J.-F. (2003). View planning for automated three-dimensional object reconstruction and inspection. ACM Computing Surveys 35(1), 64–96. https://doi.org/10.1145/641865.641868.
9. Galliani, S., Lasinger, K., Schindler, K. (2015). Massively Parallel Multiview Stereopsis by Surface Normal Diffusion. In: 2015 IEEE Int. Conf. on Computer Vision (ICCV), Santiago, pp. 873–881. https://doi.org/10.1109/ICCV.2015.106.
10. Isler, S., Sabzevari, R., Delmerico, J., Scaramuzza, D. (2016). An information gain formulation for active volumetric 3D reconstruction. In: 2016 IEEE Int. Conf. on Robotics and Automation (ICRA), Stockholm, pp. 3477–3484. https://doi.org/10.1109/ICRA.2016.7487527.
11. Vasquez-Gomez, J., Sucar, L., Murrieta-Cid, R., Lopez-Damian, E. (2014). Volumetric Next-Best-View Planning for 3D Object Reconstruction with Positioning Error. Int. J. of Advanced Robotic Syst. 11(10), 1–13. https://doi.org/10.5772/58759.
12. Alon, N., Spencer, J. (2016). The Probabilistic Method. Wiley, New York, 4th. ed.
13. Zadeh, L.A. (1965). Fuzzy sets. Information and Control 8(3), 338–353. https://doi.org/10.1016/S0019-9958(65)90241-X.
14. Pawlak, Z. (1982). Rough sets. Int. J. of Computer & Information Sciences 11(5), 341–356. https://doi.org/10.1007/BF01001956.
15. Molodtsov, D. (1999). Soft Set Theory – first results. Comput. and Math. with Appl. 37, 19–31. https://doi.org/10.1016/S0898-1221(99)00056-5.
16. Liu, S., Lin, Y. (2006). Grey Numbers and Their Operations. In: Grey Information. Advanced Information and Knowledge Processing, pp 23-43. https://doi.org/10.1007/1-84628-342-6_2.
17. Yamaguchi, D., Li, G.-D., Chen, L.-C., Nagai, M. (2007). Reviewing crisp, fuzzy, grey and rough mathematical models. In: Proc. of 2007 IEEE Int. Conf. on Grey Systems and Intelligent Services, Nanjing, China, pp. 547–552. https://doi.org/10.1109/GSIS.2007.4443334.
18. Hornung, A., Wurm, K., Bennewitz, M., Stachniss, C., Burgard, W. (2013). Octomap: An efficient probabilistic 3d mapping framework based on octrees. Autonomous Robots 34(3), 189–206. https://doi.org/10.1007/s10514-012-9321-0.
19. James, M. (2014). Flame and smoke estimation for fire detection in videos based on optical flow and neural networks. Int. J. of Research in Eng. and Technology 3(8), 324–328. https://doi.org/10.15623/ijret.2014.0308050.
20. Chen, T., Yin, Y., Huang, S., Ye, Y. (2006). The smoke detection for early fire-alarming system based on video processing. In: Proc. of 2006 Int. Conf. on Intelligent Information Hiding and Multimedia, Pasadena, CA, pp. 427–430. https://doi.org/10.5555/1193214.1193962.
21. Luo, Y., Zhao, L., Liu, P., Huang, D. (2018). Fire smoke detection algorithm based on motion characteristics and convolutional neural networks. Multimedia Tools Appl. 77(12), 15075–15092. https://doi.org/10.1007/s11042-017-5090-2.
22. Bugaric, M., Jakovcevic, T., Stipanicev, D. (2015). Computer Vision Based Measurement of Wildfire Smoke Dynamics. Advances in Electrical and Computer Engineering 15(1), 55–62. https://doi.org/10.4316/AECE.2015.01008.
23. Qiang, Y., Pei, B., Zhao, J. (2014). Forest Fire Image Intelligent Recognition based on the Neural Network. J. of Multimedia 9(3), 449–455. https://doi.org/10.4304/jmm.9.3.449-455.
24. Maturana, D., Scherer, S. (2015). VoxNet: A 3D Convolutional Neural Network for real-time object recognition. In: Proc. of 2015 IEEE/RSJ Int. Conf. on Intelligent Robots and Systems (IROS), Hamburg, pp. 922–928. https://doi.org/10.1109/IROS.2015.7353481.
25. Qian, G., Wang, H., Feng, X. (2013). Generalized hesitant fuzzy sets and their application in decision support system. Knowledge-Based Syst. 37, 357–365. https://doi.org/10.1016/j.knosys.2012.08.019.
26. Wang, Y, Dang, L, Ren, J. (2019). Forest fire image recognition based on convolutional neural network. J. of Algorithms & Computational Technology 13, 1–11. https://doi.org/10.1177/1748302619887689.
27. Tang, C., Wu, J., Hou, Y., Wang, P., Li, W. (2016). A Spectral and Spatial Approach of Coarse-to-Fine Blurred Image Region Detection. IEEE Signal Processing Letters 23(11), 1652–1656. https://doi.org/10.1109/LSP.2016.2611608.

Received 27.03.22
Accepted 22.04.22